Available online at www.sciencedirect.com

ScienceDirect

Ceramics International 40 (2014) 2891–2899

CERAMICS INTERNATIONAL

www.elsevier.com/locate/ceramint

Mechanical properties and chemical bonding characteristics of WC and W_2C compounds

YangZhen Liu[a], YeHua Jiang[a], Rong Zhou[a], Jing Feng[b,*]

[a]Faculty of Materials Science and Engineering, Kunming University of Science and Technology, Kunming, 650093, PR China
[b]School of Engineering and Applied Science, Harvard University, Cambridge, MA, 02138, USA

Received 16 August 2013; received in revised form 4 October 2013; accepted 4 October 2013
Available online 20 October 2013

Abstract

The mechanical properties and chemical bonding features of W–C binary compounds (h-WC, o-W_2C, h-W_2C and t-W_2C) were studied by density functional theory (DFT). It is shown that they are thermodynamically stable identified by the cohesive energy and formation enthalpy of W–C binary compounds. The elastic constants were calculated using the stress–strain method. The Voigt–Reuss–Hill approximation was used to evaluate the moduli. The surface constructions of bulk and Young's moduli were applied to illustrate the mechanical anisotropy. The population analysis of W–C binary compounds was used to discuss the chemical bonding, which indicate the combinations of covalent and metallic bonds in these compounds. Moreover, the anisotropic properties of sound velocities for W–C binary compounds were explored.

Keywords: C. Mechanical properties; Inorganic compounds; Anisotropy; Chemical bonding

1. Introduction

Transition metal carbides exhibit outstanding physical and chemical properties, such as extreme hardness, high melting point and high thermal conductivity. One of the most important compounds is tungsten carbide like hexagonal, orthorhombic, trigonal structure, which are the key enhanced phases in tool steels, high temperature ceramics, etc. Some theoretical works of hexagonal WC (h-WC) have been performed extensively, including the properties of bulk modulus [1–3] and stability [3,4]. Additionally, Ivanovskii et al. [5] investigated the effect of metal and carbon vacancies on the electronic structure of hexagonal WC. Cheng et al. [6] studied the thermal equation of state of tungsten carbide by first-principles calculations. The results showed that WC exhibits anisotropic linear compressibility and isotropic thermal expansion. Kurlov and Kublii [7–9] investigated the peculiarities of phase formation in tungsten–carbon as a function of W/C content and temperature by means of systematic X-ray, dilatometric and microstructural experiments. Harjinder Singh and co-workers [10] have directly synthesized the single nanocrystalline WC by scheelite and ore of tungsten (W) successfully at 800 °C. Meanwhile, the WC and W_2C are important in coatings and catalytic [11–14]. Besides, Liang et al. [15] discussed nanostructures of W_2C on ultrahigh surface carbon materials via carbothermal hydrogen reduction. Klimpel et al. [16] studied the properties of Ni–W_2C and Co–W_2C powders thermal sprayed deposits. Dash et al. [17] prepared the WC–W_2C composites of several compositions (in the range of 30–50 at% C) by arc plasma melting and in situ cooling. However, other carbides like Cr_7C_3 type multi-component carbides have been studied deeply in theory and experiments [18,19], the properties of tungsten carbides are lacked in the literatures so on. Hence, it is available to investigate the stability, mechanical anisotropy, sound velocity anisotropy and chemical bonding characteristics of W–C binary compounds. In this work, we have got these properties of WC and W_2C compounds by first-principles calculations combined empirical methods. The studied crystal structures of W–C binary compounds are shown in Fig. 1.

*Corresponding author. Tel.: +1 617 496 4295; fax: +1 857 259 2445.
E-mail address: jfeng@seas.harvard.edu (J. Feng).

0272-8842/$ - see front matter © 2013 Elsevier Ltd and Techna Group S.r.l. All rights reserved.
http://dx.doi.org/10.1016/j.ceramint.2013.10.022

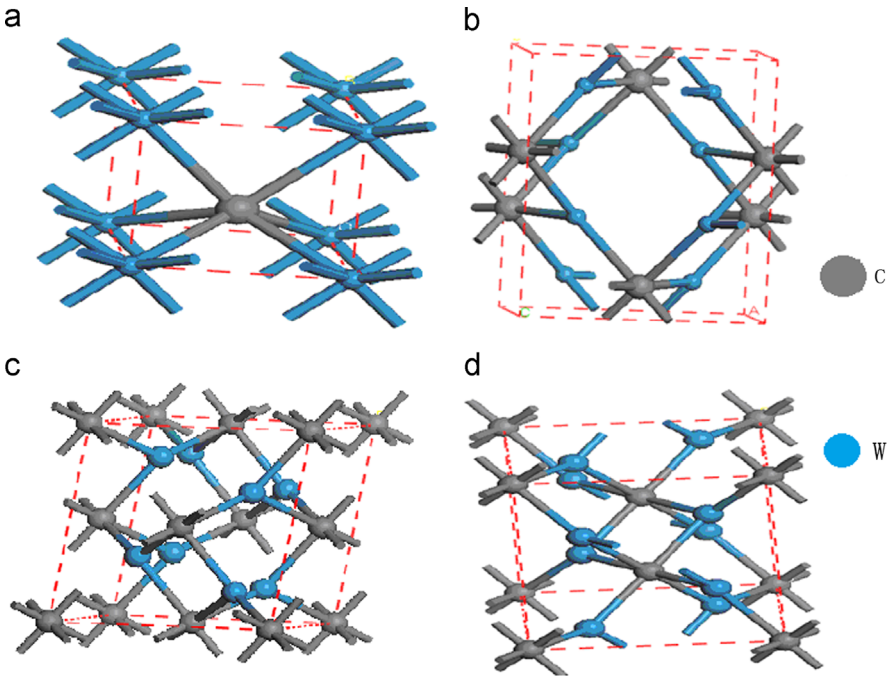

Fig. 1. Crystal structures for (a) h-WC, (b) o-W_2C, (c) h-W_2C and (d) t-W_2C compounds, respectively.

2. Methods and details

Firstly, it is worth mentioning that in unit cell of h-W_2C; the carbon atoms randomly occupy one-half of all octahedral interstices in the tungsten sublattice [7]. In the paper of Suetin [4], supercell method was used to consider the structure of h-W_2C as the uniform alternation of vacancies and carbon atoms along [001] crystal direction. Therefore, supercell method along [001] crystal direction was also used in this work.

The first-principles calculations based on density functional theory (DFT) were used to investigate the stability, mechanical anisotropy, sound velocity anisotropy and chemical bonding characteristics of h-WC, o-W_2C, h-W_2C and t-W_2C. The interactions between ionic cores and valence electrons were represented by Ultrasoft pseudopotentials. For W and C, the valence electron configurations considered are $4s^24p^64d^45s^1$, $2s^22p^2$, respectively. The exchange–correlation energy was calculated by the generalized gradient approximation (GGA) of Perdew, Burke and Ernzerhof (PBE) scheme [20]. Monkhorst–Pack scheme was used for k-point sampling in the first irreducible Brillouin zone (BZ), as $10\times10\times10$ for all structures. BFGS (Broyden–Fletcher–Goldfarb–Shannon) [21] optimized method was adopted to obtain the equilibrium crystal structures of carbides. The other convergence parameters are (1) total energy changes were reduced to 1.0×10^{-6} eV; (2) Hellman–Feynman forces acting on distinct atoms were converged less than 0.05 eV/Å. Pulay density mixing scheme was applied for the electron energy minimization process. The kinetic energy cut-off value for the plane wave expansions was selected as 450 eV. Stress–strain method was used to evaluate the elastic constants of these carbides in which several different strain modes were imposed on the crystal structure, and the Cauchy stress tensor for each strain mode was evaluated and then the related elastic constants were identified as the coefficients in strain–stress relations as shown in Eq. (1).

$$\begin{pmatrix}\sigma_1\\ \sigma_2\\ \sigma_3\\ \tau_4\\ \tau_5\\ \tau_6\end{pmatrix}=\begin{pmatrix}C_{11} & C_{12} & C_{13} & C_{14} & C_{15} & C_{16}\\ & C_{22} & C_{23} & C_{24} & C_{25} & C_{26}\\ & & C_{33} & C_{34} & C_{35} & C_{36}\\ & & & C_{44} & C_{45} & C_{46}\\ & & & & C_{55} & C_{56}\\ & & & & & C_{66}\end{pmatrix}\begin{pmatrix}\varepsilon_1\\ \varepsilon_2\\ \varepsilon_3\\ \gamma_4\\ \gamma_5\\ \gamma_6\end{pmatrix} \quad (1)$$

where, C_{ij} is the elastic constant, τ_i and σ_i are the shear stress and normal stress, respectively. The independent elements of elastic constants tensor are determined by the crystal symmetry, and for high symmetry point group, the required different strain patterns for the C_{ij} calculations can be greatly reduced, for example, one can obtain the full set elastic constants of cubic using one strain pattern.

In order to investigate the chemical stability of these compounds, the cohesive energy and formation enthalpy were calculated by the following formula:

$$E_{coh}(W_xC)=E_{tot}(W_xC)-xE_{iso}(W)-E_{iso}(C) \quad (2)$$

$$\Delta_rH(W_xC)=E_{coh}(W_xC)-xE_{coh}(W)-E_{coh}(C) \quad (3)$$

where $E_{coh}(X)$ and $\Delta_rH(X)$ are the cohesive energy and formation enthalpy of X compounds, respectively; $E_{tot}(X)$ is the total energy of X and $E_{iso}(X)$ refers to the total energy of a single X atom.

3. Results and discussions

3.1. Stability

The calculated lattice parameters, cohesive energy and formation enthalpy of h-WC, o-W_2C, h-W_2C and t-W_2C compounds are listed in Table 1, respectively. Because of GGA used in our work, the lattice parameters of W–C binary compounds may be overestimated. Moreover, the chemical stability of these compounds can be described by cohesive energy and formation enthalpy. As shown in Table 1, the cohesive energies of W–C compounds are negative values, and the values of cohesive energy are −10.65 eV/atom, −10.91 eV/atom, −10.93 eV/atom and −10.90 eV/atom for h-WC, o-W_2C, h-W_2C and t-W_2C, respectively. Therefore, h-W_2C is more stable than other carbides in the case of cohesive energy. However, the stability of compound is determined by formation enthalpy (Eq. (3)), the lower the formation enthalpy, the more stable the compound. The values of formation enthalpy for h-WC, o-W_2C, h-W_2C and t-W_2C are −0.118 eV/atom, −0.019 eV/atom, −0.027 eV/atom and −0.007 eV/atom, respectively. The following sequence of the stability in W–C system is as follows: h-WC > h-W_2C > o-W_2C > t-W_2C, which is consistent with the result of Li et al. [22]. Hence, the most stable compound among them is the h-WC.

3.2. Elastic constants and polycrystalline moduli

The elastic constants of carbides play an important role in the application like wear resistance material. In this work, the elastic constants of h-WC, o-W_2C, h-W_2C and t-W_2C compounds are calculated by stress–strain approach and the results are listed in Table 2, while the calculated elastic compliance matrices are presented in Table 3. According to Born–Huang's lattice dynamical theory, the mechanical stability criterions can be expressed as [23,24]:

Table 1
The calculated lattice parameters (a, b, c in Å) and cohesive energy (eV/atom) and formation enthalpy (eV/atom) of h-WC, o-W_2C, h-W_2C and t-W_2C.

Phase	h-WC	o-W_2C	h-W_2C	t-W_2C
Space group	P−6m2	Pbcn	P63/mmc	P−31m
a	2.923 (2.906[a])	4.756 (4.728[a])	2.995 (3.002[a])	5.235 (5.184[a])
b	2.923 (2.906[a])	6.093 (6.009[a])	5.993	5.235 (5.184[a])
c	2.841 (2.837[a])	5.244 (5.193[a])	4.792 (4.75[a])	4.777 (4.721[a])
Cohesive energy	−10.65	−10.91	−10.93	−10.90
Formation enthalpy	−0.118(−0.106[b])	−0.019(−0.018[b])	−0.027(−0.029[b])	−0.007(−0.003[b])

[a]Exp. in Ref. [7].
[b]Cal. in Ref. [22].

Table 2
The calculated independent elastic constants (C_{ij}, in GPa) of h-WC, o-W_2C, h-W_2C and t-W_2C compounds using the stress-strain method.

Species	C_{ij}								
	C_{11}	C_{12}	C_{13}	C_{22}	C_{23}	C_{33}	C_{44}	C_{55}	C_{66}
h-WC	715.1 (772.8[a] 720[b])	211.7 (209.9[a] 254[b])	163.3 (157.8[a] 267[b])	–	–	959.4 (960.6[a] 972[b])	301.2 (302.2[a] 328[b])	–	–
o-W_2C	507.7	240.9	251.8	537.6	175.4	529.1	163.3	194.8	212.9
h-W_2C	578.9	183.3	223.5	–	–	527.1	211.8	–	–
t-W_2C	534.2	197.5	267.9	–	–	498.0	202.4	–	–

[a]Calculated by FLAPW with GGA scheme in Ref. [25].
[b]Exp. in Ref. [26].

Table 3
The elastic compliance matrix of h-WC, o-W_2C, h-W_2C and t-W_2C compounds.

Species	S_{ij}								
	S_{11}	S_{12}	S_{13}	S_{22}	S_{23}	S_{33}	S_{44}	S_{55}	S_{66}
h-WC	0.00156	−0.00042	−0.00020	0.00156	−0.00020	0.00111	0.00332	0.00332	0.00397
o-W_2C	0.00298	−0.00098	−0.00109	0.00241	−0.00033	0.00252	0.00613	0.00513	0.00470
h-W_2C	0.00215	−0.00039	−0.00074	0.00215	−0.00074	0.00263	0.00475	0.00475	0.00507
t-W_2C	0.00262	−0.00036	−0.00121	0.0026	−0.00121	0.00331	0.00495	0.00495	0.00595

For hexagonal system (h-WC and h-W_2C):

$$C_{11}>0,\quad C_{44}>0,\quad C_{11}-C_{12}>0,$$
$$(C_{11}+C_{12})C_{33}-2C_{13}^2>0 \tag{4}$$

For orthorhombic system (o-W_2C):

$$C_{11}+C_{12}+C_{33}+2C_{12}+2C_{13}+2C_{23}>0,$$
$$C_{11}+C_{22}>2C_{12}, C_{22}+C_{33}>2C_{23},$$
$$C_{11}+C_{33}>2C_{13}, C_{ii}>0\quad (i=1-6) \tag{5}$$

For trigonal system (t-W_2C):

$$C_{11}>|C_{12}|, (C_{11}+C_{12})C_{33}>2C_{13}^2,$$
$$(C_{11}-C_{12})C_{44}-2C_{14}^2>0 \tag{6}$$

From Table 2, it is obvious that the calculated elastic constants of h-WC, o-W_2C, h-W_2C and t-W_2C compounds satisfy the corresponding criterions, respectively, which imply that they are mechanically stable. Moreover, the results are coincided with other theoretical and experimental results [25,26]. For these compounds, C_{11} and C_{33} are larger than other elastic constants, which indicate that they are very incompressible under uniaxial stress along $x(\varepsilon_{11})$ or $z(\varepsilon_{33})$ axis. C_{44} illustrates the resistance of the crystal with respect to the shear strain at (100) plane, and which is closely related to the shear modulus. As can be seen from Table 2, h-WC has the highest C_{44} in W–C binary system.

Bulk modulus reflects the compressibility of the solid under hydrostatic pressure. The bulk modulus (B), Young's modulus (E) and shear modulus (G) can be calculated using Voigt–Reuss–Hill (VRH) approximation. The VRH is an average of the two bounds, namely lower bound of Voigt and upper bound of Reuss, which provides the best estimation for mechanical properties of polycrystalline materials from the known elastic constants of single crystal. They can be obtained by the Eqs. (7)–(10) [22]:

$$B_{VRH}=\frac{1}{2}(B_V+B_R) \tag{7}$$

$$G_{VRH}=\frac{1}{2}(G_V+G_R) \tag{8}$$

$$E=\frac{9B_{VRH}G_{VRH}}{(3B_{VRH}+G_{VRH})} \tag{9}$$

$$\delta=\frac{(3B_{VRH}-2G_{VRH})}{[2(3B_{VRH}+G_{VRH})]} \tag{10}$$

where B_V, B_R and B_{VRH} are the bulk modulus calculated by Voigt, Reuss and Voigt–Reuss–Hill approximation, respectively. G_V, G_R and G_{VRH} are the shear modulus calculated within Voigt, Reuss and Voigt–Reuss–Hill approximation, respectively. E is Young's modulus and δ is Poisson's ratio, which is calculated by VRH method. The calculated formulas in VRH method are dependent on the crystal symmetry, and listed in the references [27,28]. The values of B, G, E and Poisson's ratio (δ) for h-WC, o-W_2C, h-W_2C and t-W_2C compounds are presented in Table 4, which are in good agreement with other theoretical results [25]. It can be seen that h-WC has the maximum values of B; G and E; with the values 383.2 GPa, 291.2 GPa and 697 GPa, respectively. Correlation between hardness and elastic moduli of the covalent crystals were studied by Jiang [29], and the results show that the compound with large values of B, G and E should be of large hardness. Therefore, it can be seen that the hardness of h-WC may be the largest among them. Furthermore, the ratio of B/G is generally used to indicate the compound with ductility or brittleness. It is reported that the brittle compound, B/G is smaller than 1.75. On the contrary, it more likes ductile compound. The hardness and brittleness of the compound may be related to the B/G value, the higher hardness of compound usually has smaller B/G value. The B/G value of h-WC, o-W_2C, h-W_2C and t-W_2C is 1.32, 1.88, 1.73 and 2.03, respectively. Thus, the h-WC should be more brittle and larger hardness than other carbides, which is consistent with above discussions.

As we all know, microcracks are easily caused in materials, which are mainly in that the significant elastic anisotropy [30]. Therefore, the elastic anisotropy is important to improve their durability. Nevertheless, the elastic anisotropy of a crystal can be characterized by many different ways. In this work, the universal anisotropic index (A^U) and percent anisotropy (A_B and A_G) can be calculated by the following equations [31]:

$$A^U=5\frac{G_V}{G_R}+\frac{B_V}{B_R}-6\geq 0 \tag{11}$$

$$A_B=\frac{B_V-B_R}{B_V+B_R} \tag{12}$$

$$A_G=\frac{G_V-G_R}{G_V+G_R} \tag{13}$$

If the indexes in Eqs. (11)–(13) are zero, it would be an isotropic structure. The large deviations from zero refer to the highly anisotropic mechanical properties. The shear anisotropic factor A_1 is defined as by Xiao et al. [18]:

$$A_1=\frac{4C_{44}}{C_{11}+C_{33}-2C_{13}} \tag{14}$$

Table 4
The calculated mechanical moduli of h-WC, o-W_2C, h-W_2C and t-W_2C compounds, including bulk moduli (B_V, B_R and B_{VRH}), shear moduli (G_V, G_R and G_{VRH}), Young's modulus (E) (in GPa) and Poisson's ratio (δ).

Species	B_V	B_R	G_V	G_R	B_{VRH}	G_{VRH}	E	δ
h-WC	385.1 (384.2[a])	381.3 (380.7[a])	294.2 (297.5[a])	288.2 (291.7[a])	383.2 (382.4[a])	291.2 (294.6[a])	697.0 (703.2[a])	0.197 (0.194[a])
o-W_2C	323.4	322.8	174.6	168.4	323.1	171.5	437.2	0.275
h-W_2C	330.7	330.5	193.5	187.7	330.6	190.6	479.6	0.258
t-W_2C	337.0	336.7	170.2	161.5	336.8	165.8	427.3	0.289

[a]Calculated by FLAPW with GGA scheme in Ref. [25].

The results are shown in Table 5, which imply that the t-W_2C has the largest value of A^U among these compounds. The values of A_B for o-W_2C, h-W_2C and t-W_2C are very small (0.001), indicating that these compounds do not show strong anisotropy in bulk modulus. A_G and A_1 determine the anisotropy of shear modulus, but the value of A_1 is quite different from A_G. The value of A_1 seems to support the hypothesis that the shear modulus of W–C system has a strong directional dependence. The universal anisotropic index (A^U) is a better indicator for mechanical anisotropic properties. The larger the value A^U is, the stronger the anisotropy of the compound is.

Table 5
The calculated universal anisotropic index (A^U), percent anisotropy (A_G and A_B) and shear anisotropic factors (A_1) of h-WC, o-W_2C, h-W_2C and t-W_2C compounds.

Species	A^U	A_B	A_G	A_1
h-WC	0.114	0.005	0.010	0.894
o-W_2C	0.186	0.001	0.018	1.225
h-W_2C	0.155	0.001	0.015	1.286
t-W_2C	0.270	0.001	0.026	1.631

However, the simplest way to illustrate the anisotropy of mechanical moduli is to plot them in three dimensions as a function of crystallographic orientation. Here, the bulk modulus and Young's modulus on different directions using spherical coordinates are plotted. The directional dependent

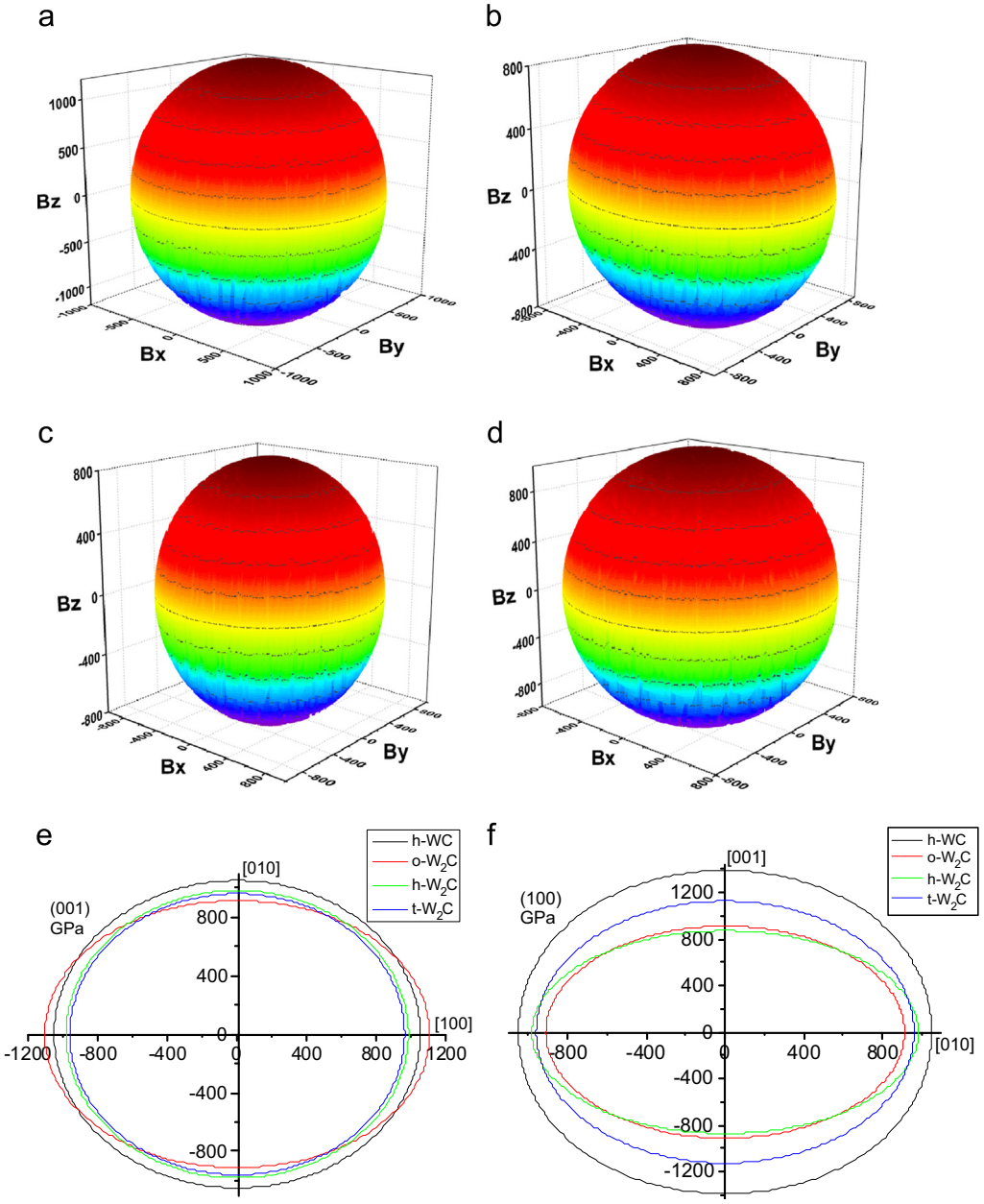

Fig. 2. (a–d) The surface construction of bulk modulus of W–C system. (e and f) The (001) and (100) plane projections of bulk modulus for the W–C binary system, respectively. (a) h-WC, (b) o-W_2C, (c) h-W_2C, (d) t-W_2C, (e) the (001) crystal plane and (f) the (100) crystal plane.

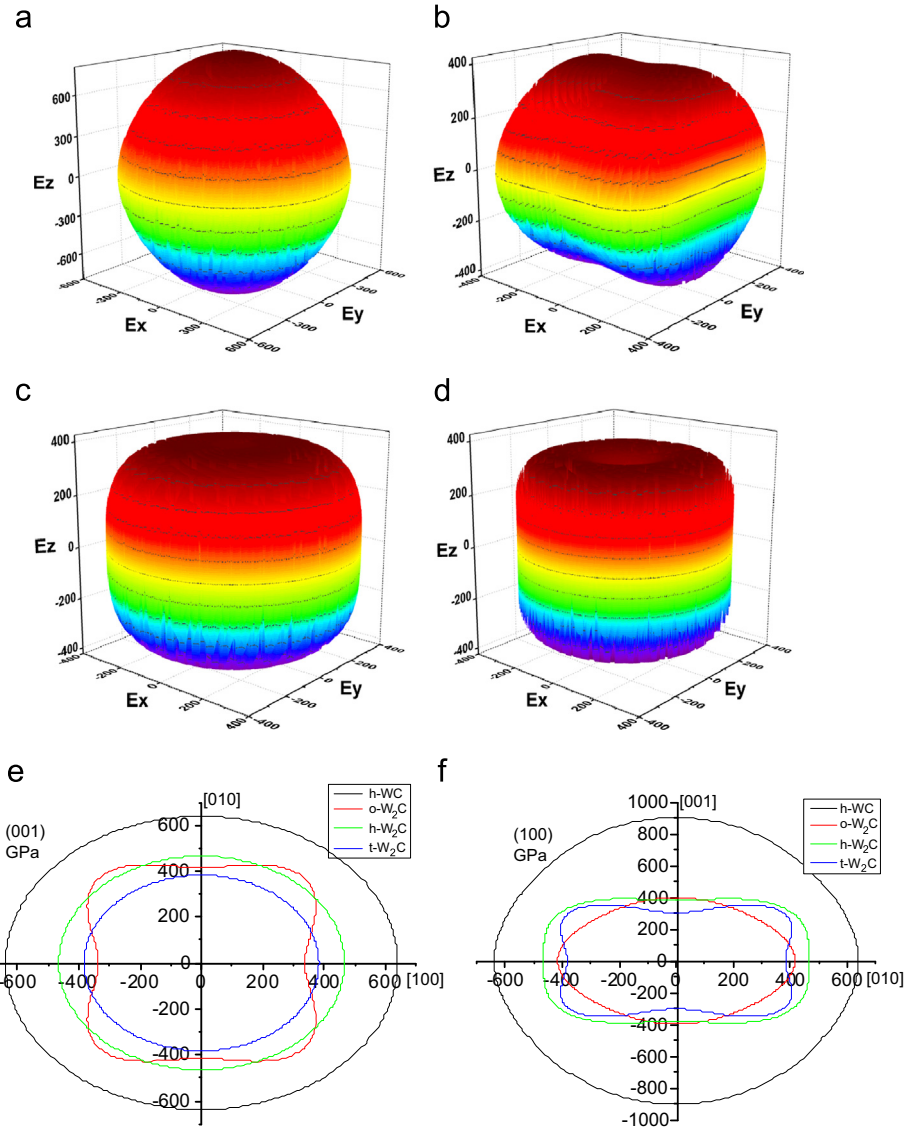

Fig. 3. (a–d) The directional dependence of Young's modulus for W–C system. The projections of Young's modulus for the W–C binary system at (e) (001) crystal plane and (f) (100) plane. (a) h-WC, (b) o-W_2C, (c) h-W_2C, (d) t-W_2C, (e) the (001) crystal plane and (f) the (100) crystal plane.

of B and E can be written as follows:

$$\frac{1}{B} = (S_{11}+S_{12}+S_{13})l_1^2+(S_{12}+S_{22}+S_{23})l_2^2+(S_{13}+S_{23}+S_{33})l_3^2 \tag{15}$$

$$\frac{1}{E} = l_1^4S_{11}+2l_1^2l_2^2S_{12}+2l_1^2l_3^2S_{13}+l_2^4S_{22}+2l_2^2l_3^2S_{23}+l_3^4S_{33} + l_2^2l_3^2S_{44}+l_1^2l_3^2S_{55}+l_1^2l_2^2S_{66} \tag{16}$$

where S_{ij} are the elastic compliance constants, l_1, l_2 and l_3 are the directional cosines. The bulk modulus of h-WC, o-W_2C, h-W_2C and t-W_2C compounds on different directions by the model of spherical coordinates, and the (001) and (100) plane projections of bulk modulus for W–C binary compounds are shown in Fig. 2. It can be seen that the bulk moduli of W–C binary compounds show weak anisotropy from Fig. 2. The projections on the (001) and (100) planes indicate more details about the anisotropic properties of bulk modulus. Fig. 3 shows the directional dependence of E for W–C binary compounds, and the projections of Young's modulus for W–C binary compounds at (e): (001) crystal plane and (f): (100) plane. As can be seen from Fig. 3, the projections of Young's modulus on the (100) and (001) planes show more anisotropic features, compared with bulk modulus. Therefore, Young's modulus has a stronger directional dependence on this plane. Additionally, the calculated anisotropic indexes and factors are in good agreement with the above discussions.

3.3. Mulliken population analysis

The calculated chemical bonding characteristics of tungsten carbides are listed in Table 6; the average bond length and the

Table 6
Mulliken population analysis results of the studied carbides (the average bond length and average bond population).

Species	Bond	$\overline{L}(AB)$ (Å)	$\overline{n}_{AB}$ (e)	Net overlap electrons
h-WC	C–W	2.21	2.11	2.11
o-W_2C	C–W	2.11	0.30	7.2
	W–W	2.95	0.20	3.2
	C–C	2.99	−0.08	−0.16
h-W_2C	C–W	2.12	0.34	9.12
	W–W	2.94	0.29	3.48
t-W_2C	C–W	2.12	0.26	4.68
	W–W	2.93	0.15	1.35

bond population are calculated using the Eqs. (17) and (18) [32]:

$$\overline{L}(AB) = \frac{\sum_i L_i N_i}{\sum_i N_i} \tag{17}$$

$$\overline{n}_{AB} = \frac{\sum_i n_i^{AB} N_i}{\sum_i N_i} \tag{18}$$

here $\overline{L}(AB)$ and $\overline{n}_{AB}$ represent the average bond length and the bond population, respectively; N_i is the total number of i bond in the cell and L_i is the bond length of i type. On one hand, C atoms carry the negative charges for all of carbides, and the value range from −0.6e (h-WC) to −0.71e (t-W_2C). On the other hand, the largest positive charges are carried by W atoms of h-WC among these carbides. As shown in Table 6, the net bonding electrons of the h-W_2C increase to 12.6e/cell, which is larger than that of other carbides. However, the smallest value of the net bonding electrons is h-WC (2.11e/cell), which shows that it is less stable than other carbides. From the above discussions, the cohesive energy values of h-WC, o-W_2C, h-W_2C and t-W_2C are −10.65 eV/atom, −10.91 eV/atom, −10.93 eV/atom and −10.90 eV/atom, respectively, which are in agreement with the Mulliken population analysis. Furthermore, W–W bonds show the positive overlap populations, implying metallic bonding character between tungsten atoms. For o-W_2C, C–C bonds have negative overlap populations, indicating anti-bond states or strong electrostatic repulsion among carbon atoms. A high value of the bond population indicates a covalent bond in these compounds [33]. Therefore, the covalent bond is mainly determined by C–W bonds for all compounds. Based on above discussions, it can be seen that the combinations of covalent and metallic bonds are the main bonding characteristic in WC and W_2C compounds.

3.4. Debye temperature and anisotropic sound velocity

The Debye temperature is a fundamental parameter of a material, linked to many physical properties such as specific heat, elastic constants and melting point [34]. The Debye temperature (Θ_D) can be estimated from the average sound velocity v_m, the expressions are given by Eqs. (19)–(22) [35]:

$$\Theta_D = \frac{h}{k}\left[\frac{3n}{4\pi}\left(\frac{N_A\rho}{M}\right)\right]^{1/3} \nu_m \tag{19}$$

where h is Planck's constant, k is the Boltzmann constant, N_A is Avagadro's constant, n is the number of atoms in the molecule, M is the molecular weight, and ρ is the theoretical density of the compound. The average sound velocity v_m can be calculated from:

$$\nu_m = \left[\frac{1}{3}\left(\frac{2}{\nu_t^3} + \frac{1}{\nu_l^3}\right)\right]^{-(1/3)} \tag{20}$$

$$\nu_l = \sqrt{\frac{(B+(4/3)G)}{\rho}} \tag{21}$$

$$\nu_t = \sqrt{\frac{G}{\rho}} \tag{22}$$

here B and G are the bulk and shear modulus, respectively. v_l is the longitudinal sound velocity and v_t is the transverse sound velocity. The Debye temperature and sound velocities of W–C binary compounds are shown in Table 7. Debye temperature reflects the strength of chemical bonding in the crystal structure and which is inverse to the molecular weight. As can be seen from Table 7, the Debye temperature of h-WC is larger than that of other carbides, which indicate that the covalent bonding in h-WC is stronger than other carbides. Both v_l and v_t are related to the bulk modulus and density, the compound with low density and high bulk modulus have large sound velocity. The h-WC has the largest sound velocity among W–C binary compounds, because it has smaller density and larger bulk modulus. The pure transverse and longitudinal modes can be only found for [100], [010] and [001] directions in an orthorhombic crystal and the sound propagating modes in other directions are the quasi-transverse or quasi-longitudinal waves. In this work, we only consider the pure propagating modes for W–C binary compounds: [100] and [001] directions for hexagonal and trigonal crystal; [100], [010] and [001] directions for orthorhombic crystal. On different directions for crystals, the sound velocities can be written as: [35]

Hexagonal and trigonal crystal class:

$$\begin{aligned} &[100] \\ &[100]v_i = \sqrt{(C_{11}-C_{12})/2\rho}; \\ &[010]v_{t1} = \sqrt{C_{11}/\rho}; \\ &[001]v_{t2} = \sqrt{C_{44}/\rho} \end{aligned} \tag{23}$$

Table 7
Sound velocities and Debye temperature of h-WC, o-W_2C, h-W_2C and t-W_2C compounds.

Species	ρ (g/cm^3)	v_l (m/s)	v_t (m/s)	v_m (m/s)	Θ_D (K)
h-WC	15.47	7061.8	4338.6	4788.1	650.4
o-W_2C	16.60	5765.3	3214.2	3578.8	456.9
h-W_2C	16.47	5958.4	3401.8	3780.3	481.2
t-W_2C	16.59	5798.8	3161.3	3526.0	449.9

Table 8
The anisotropic sound velocities of hexagonal WC and W_2C, orthorhombic W_2C and trigonal W_2C compounds, and the unit of velocity (v) is km/s.

Direction	[100]			[010]			[001]		
	$[100]v_l$	$[010]v_{t1}$	$[001]v_{t2}$	$[010]v_l$	$[100]v_{t1}$	$[001]v_{t2}$	$[001]v_l$	$[100]v_{t1}$	$[010]v_{t2}$
h-WC	4.034	6.799	4.412	–	–	–	4.412	7.875	4.412
o-W_2C	5.530	3.581	3.426	5.691	3.581	3.136	5.646	3.426	3.136
h-W_2C	3.466	5.928	3.586	–	–	–	3.586	5.657	3.586
t-W_2C	3.186	5.675	3.493	–	–	–	3.493	5.479	3.493

[001]

$$[001]v_l = \sqrt{C_{44}/\rho};$$
$$[100]v_{t1} = \sqrt{C_{33}/\rho};$$
$$[010]v_{t2} = \sqrt{C_{44}/\rho} \quad (24)$$

Orthorhombic crystal class:

[100]

$$[100]v_l = \sqrt{C_{11}/\rho},$$
$$[010]v_{t1} = \sqrt{C_{66}/\rho},$$
$$[001]v_{t2} = \sqrt{C_{55}/\rho} \quad (25)$$

[010]

$$[010]v_l = \sqrt{C_{22}/\rho},$$
$$[100]v_{t1} = \sqrt{C_{66}/\rho},$$
$$[001]v_{t2} = \sqrt{C_{44}/\rho} \quad (26)$$

[001]

$$[001]v_l = \sqrt{C_{33}/\rho},$$
$$[100]v_{t1} = \sqrt{C_{55}/\rho},$$
$$[010]v_{t2} = \sqrt{C_{44}/\rho} \quad (27)$$

where v is the sound velocity (v_l: the longitudinal wave of sound velocity, v_{t1}: the first transverse wave of sound velocity, v_{t2}: the second transverse of sound velocity). The calculated results are presented in Table 8.

4. Conclusions

By performing the first principles calculations based on density functional theory (DFT), the stability, mechanical anisotropy, chemical bonding characteristics and sound velocity anisotropy of W–C binary compounds (h-WC, o-W_2C, h-W_2C and t-W_2C) are studied in this work. The cohesive energy and formation enthalpy of these compounds are calculated and the results reveal they are thermodynamically stable ($E_{form} < 0$). The calculated elastic constants satisfy the Born–Huang's stability criterions, which imply that these compounds are mechanically stable. The mechanical moduli are obtained from the elastic constants using Voigt–Reuss–Hill approximation. The results indicate that the values of bulk modulus, shear modulus and Young's modulus for h-WC are larger than others, implying that the hardness of h-WC is the largest among them. Besides, the h-WC should be more brittle than other carbides. Several anisotropic indexes and factors are calculated to illustrate the mechanical anisotropy. The results show that Young's modulus of these compounds has strong anisotropic property while the bulk modulus has a relatively weak directional dependent. The 3D surface constructions of bulk modulus and Young's modulus are plotted to show their anisotropies. The Mulliken population for the chemical bonds of these compounds is estimated. The results indicate the combinations of covalent and metallic bonds in these compounds.

Acknowledgments

This work is supported by National Natural Science Foundation of China (Nos. 51171074 and 51261013).

References

[1] L.F. Mattheiss, D.R. Hamann, Bulk and surface electronic structure of hexagonal WC, Phys. Rev. B 30 (1984) 1731–1738.
[2] V.P. Zhukov, V.A. Gubanov, Energy-band structure and thermo-mechanical properties of tungsten and tungsten carbides as studied by the LMTO-ASA method, Solid State Commun. 56 (1985) 51–55.
[3] A.Y. Liu, R.M. Wentzcovitsh, M.L. Cohen, Structural and electronic properties of WC, Phys. Rev. B 38 (1988) 9483–9489.
[4] D.V. Suetin, I.R. Shein, A.L. Ivanovskii, Structural, electronic properties and stability of tungsten mono- and semi-carbides: A first principles investigation, J. Phys. Chem. Solids 70 (2009) 64–71.
[5] A.L. Ivanovskii, N.I. Medvedeva, Effect of metal and carbon vacancies on the electronic structure of hexagonal WC and cubic TaC, Mendeleev Commun. 1 (2001) 10–12.
[6] X.Y. Cheng, J.H. Zhou, X. Xiong, Y. Du, C. Jiang, First-principles thermal equation of state of tungsten carbide, Comput. Mater. Sci. 59 (2012) 41–47.
[7] A.S. Kurlov, A.I. Gusev, Phase equilibria in the W–C system and tungsten carbides, Russ. Chem. Rev. 75 (2006) 617–636.
[8] A.S. Kurlov, A.I. Gusev, Neutron and X-ray diffraction study and symmetry analysis of phase transformations in lower tungsten carbide W_2C, Phys. Rev. B 76 (2007) 174115–174131.
[9] V.Z. Kublii, T.Y. Velikanova, Structural studies of materials-ordering in the carbide W_2C and phase equilibria in the tungsten–carbon system in the region of its existence, Powder Metall. Metal Ceram. 43 (2004) 630–644.
[10] Harjinder Singh, O.P. Pandey, Single step synthesis of tungsten carbide (WC) nanoparticles from scheelite ore, Ceram. Int. 39 (2013) 6703–6706.
[11] T. Li, Q. Li, J.Y.H. Fuh, P.C. Yu, C.C. Wu, Effects of lower cobalt binder concentrations in sintering of tungsten carbide, Mater. Sci. Eng. A 430 (2006) 113–119.

[12] M.F. Morks, Y. Gao, N.F. Fahim, F.U. Yinquing, Microstructure and hardness properties of cermet coating sprayed by low plasma, Mater. Lett. 60 (2006) 1049–1053.
[13] M.K. Neylon, S. Choi, H. Kwon, K.E. Curry, L.T. Thompson, Catalytic properties of early transition metal nitrides and carbides: n-butane hydrogenolysis, dehydrogenation and isomerization, Appl. Catal. A 183 (1999) 253–263.
[14] Y. Ishikawa, H. Jinbo, H. Yamanaka, Effect of tungsten on systhesis of multiwalled carbon nanotubes using cobalt as catalyst, Jpn. J. Appl. Phys. 45 (2006) L50–L53.
[15] C.H. Liang, F.P. Tian, Z.B. Wei, Q. Xin, C. Li, The synthesis of nanostructured W_2C on ultrahigh surface area carbon materials via carbothermal hydrogen reduction, Nanotechnology 14 (2003) 955–958.
[16] A. Klimpel, L.A. Dobrzanski, A. Lisiecki, D. Janicki, The study of properties of Ni–W_2C and Co–W_2C powders thermal sprayed deposits, J. Mater. Process. Technol. 164 (2005) 1068–1073.
[17] T. Dash, B.B. Nayak, Preparation of WC–W_2C composites by arc plasma melting and their characterizations, Ceram. Int. 39 (2013) 3279–3292.
[18] B. Xiao, J. Feng, C.T. Zhou, Y.H. Jiang, R. Zhou, Mechanical properties and chemical bonding characteristics of Cr_7C_3 type multicomponent carbides, J. Appl. Phys. 109 (2011) 023507.
[19] J. Feng, B. Xiao, R. Zhou, W. Pan, D.R. Clarke, Anisotropic elastic and thermal properties of the double perovskite slab-rock salt layer $Ln_2SrAl_2O_7$ natural superlattice structure, Acta Mater. 60 (2012) 3380–3392.
[20] J.P. Perdew, K. Burke, M. Ernzerhof, Generalized gradient approximation made simple, Phys. Rev. Lett. 77 (1996) 3865–3868.
[21] B.G. Pfrommer, M. Cote, S.G. Louie, M.L. Cohen, Relaxation of crystals with the quasi-newton method, J. Comput. Phys. 131 (1997) 233–240.
[22] Y.F. Li, Y.M. Gao, B. Xiao, T. Min, Z.J. Fan, S.Q. Ma, L.L. Xu, Theoretical study on the stability, elasticity, hardness and electronic structures of W–C binary compounds, J. Alloys Compd. 502 (2010) 28–37.
[23] S.K.R. Patil, S.V. Khare, B.R. Tuttle, J.K. Bording, S. Odambaka, Mechanical stability of possible structures of PtN investigated using first-principles calculations, Phys. Rev. B 73 (2006) 104118.
[24] Z.J. Wu, E.J. Zhao, H.P. Xiang, X.F. Hao, X.J. Liu, J. Meng, Crystal structures and elastic properties of superhard IrN_2 and IrN_3 from first principles, Phys. Rev. B 76 (2007) 054115–054130.
[25] D.V. Suetin, I.R. Shein, A.L. Ivanovskii, Elastic and electronic properties of hexagonal and cubic polymorphs of tungsten monocarbide WC and mononitride WN from first-principles calculations, Phys. Status Solidi B 245 (2008) 1590–1597.
[26] M. Lee, R.S. Gilmore, Single crystal elastic constants of tungsten monocarbide, J. Mater. Sci. 17 (1982) 2657–2660.
[27] Y.F. Mo, M.J. Pang, W.C. Yang, Y.Z. Zhan, Effects of alloying elements on structural, electronic and mechanical properties of $AlSc_2$ by first-principles calculations, Comput. Mater. Sci. 69 (2012) 160–167.
[28] Z.C. Huang, J. Feng, W. Pan, First-principles calculations of mechanical and thermodynamic properties of $YAlO_3$, Comput. Mater. Sci. 50 (2011) 3056–3062.
[29] X. Jiang, J.J. Zhao, X. Jiang, Correlation between hardness and elastic moduli of the covalent crystals, Comput. Mater. Sci. 50 (2011) 2287–2290.
[30] P. Ravindran, L. Fast, P.A. Korzhavyi, B. Johansson, J. Wills, O. Eriksson, Density functional theory for calculation of elastic properties of orthorhombic crystals: application to $TiSi_2$, J. Appl. Phys. 84 (1998) 4891–4904.
[31] J. Feng, B. Xiao, C.L. Wan, Z.X. Qu, Z.C. Huang, J.C. Chen, R. Zhou, W. Pan, Electronic structure, mechanical properties and thermal conductivity of $Ln_2Zr_2O_7$ (Ln=La, Pr, Nd, Sm, Eu and Gd) pyrochlore, Acta. Mater. 59 (2011) 1742–1760.
[32] B. Xiao, J.D. Xing, J. Feng, C.T. Zhou, Y.F. Li, W. Su, X.J. Xie, Y.H. Chen, A comparative study of Cr_7C_3, Fe_3C and Fe_2B in cast iron both from A_B initio calculations and experiments, J. Phys. D. Appl. Phys. 42 (2009) 115415–115431.
[33] C.L. Li, Z.Q. Wang, C.Y. Wang, Phase stability, mechanical properties and electronic structure of hexagonal and trigonal $Ti_5Al_2C_3$: an A_B initio study, Intermetallics 33 (2013) 105–112.
[34] J.M. Wang, J.F. Sun, Elastic and thermodynamic properties of IrN_2 under pressure, Phys. Status Solidi B 247 (2010) 921–926.
[35] J. Feng, B. Xiao, J. Chen, Y. Du, J. Yu, R. Zhou, Stability, thermal and mechanical properties of Pt_xAl_y compounds, Mater. Des. 32 (2011) 3231–3239.